

Electronic Supplementary Information

Kinetic Monte Carlo simulations on electroforming in nanomanipulated conductive bridge random access memory devices

Yu-Chen Li,^a Ping Xu,^b Yang-Yang Lv,^{c,d} Wei Fa,^b and Shuang Chen^{a,*}

^aKuang Yaming Honors School, Nanjing University, Nanjing, Jiangsu 210023, China

^bNational Laboratory of Solid State Microstructures and Department of Physics, Nanjing University, Nanjing, Jiangsu 210093, China

^dNational Laboratory of Solid State Microstructures and Department of Materials Science and Engineering, Nanjing University, Nanjing, Jiangsu 210023, China

^dKey Laboratory of Quantum Materials and Devices of Ministry of Education Southeast University, Nanjing, Jiangsu 211189, China

Email: chenshuang@nju.edu.cn

S1. Kinetic Monte Carlo (KMC) treatment and parameter illustration

In our previous KMC simulations on Ag/inhomogeneous SiO₂/Pt conductive bridge random access memories (CBRAMs), the KMC modeling was established.¹ In order to perform systematic investigations on our newly proposed nanomanipulation strategies here, the previous KMC modeling should be further modified. The most significant difference is to induce the nanopore-containing ion-blocking layers (IBLs) here. The simulated electrochemical metallization (ECM) cells were also built based on two-dimensional (2D) grids in **Fig. 1b**. These ECM cells possess two-terminal architecture of active metal electrode (in red)/nanopore-containing IBL (in black)/dielectric (in grey and white)/inert metal electrode (in blue). The anode, cathode, and IBL are represented by a one-grid thick layer separately, and they are unchanged in the following KMC simulations. The red anode is modelled as an ideal source of active metals, which can randomly release active metals when being chosen to execute these releasing KMC steps. Due to the existence of IBL here, the released active metals can only appear in the nanopores of IBL, different from our previous KMC modeling.¹ The nanopore in IBL was expressed as void or non-void sites like dielectric to allow active metals to occupy. The 2D 100×100 grids were used to stand for the dielectric layer with its void concentration equal to c . The size of each grid is 0.2 nm in **Table 1**, sufficiently considering the size of an active metal like Ag. Initially, the void sites were randomly chosen in these 2D grids. During the conductive filament growth, the void versus non-void sides can dynamically evolve with the fixed void concentration. The active metals can be oxidized to enter the dielectric layer through the nanopore in IBL. Then, they can diffuse in the dielectric layer or on the electrode surfaces, be reduced to grow clusters or filaments at any site within the dielectric layer, or be absorbed or desorbed to/from the grown clusters or filaments.

As discussed above, the KMC events involving behaviors of active metals in ECM systems can be classified into their reduction/oxidation reactions at the electrode/dielectric

layer interfaces, ion migration, absorption/desorption to/from the active metal clusters or electrode surfaces, and surface diffusion. Except reactions at the interfaces, all the other events should be distinguished involving void sites versus non-void sites. Hence, the activation energy values (expressed as $E_{x,y-y}$) related to these events can be divided into 12 different types in **Table S1**. These events follow the activation-energy-based Arrhenius relationship to determine their possibility to happen or not in our KMC procedure in **Fig. 2**. Their exact values were chosen referring to the previous 2D-gridded KMC simulations on similar ECM cells.^{1, 2} The most improvement for our built KMC modeling is to distinguish void versus non-void sites to represent the inhomogeneity of real dielectric layers.¹ From our previous modeling¹ to here, one more important modification for these KMC parameters is to correct conductivities for active metal or the dielectric layer to approach to the real situation further, as illustrated in **Table S1**. The grown filaments are of nanometer size to determine their smaller conductivity compared to that of the metal bulk. With referring to the conductivities of doped-free Si ($\sim 10^{-1}$ S/m)³ or SiO₂ ($< 10^{-12}$ S/m)⁴, the conductivity of dielectric layer was reset as small as about 10^{-6} S/m.

The detailed physical significance of most KMC parameters can be found in our previous study.¹ In brief, the KMC parameter setting here mainly depends on the inhomogeneity of the dielectric layer to distinguish void and non-void sites and the judgement of whether active metals undergo nucleation or not. Significantly, the diffusion rates of active metals on void versus non-void sites should be set to be quite different. The status of active metals for nucleation or not can be expressed as absorption/desorption of a certain active metal to/from the grown clusters or filaments. Considering the real growth situation, the grown clusters/filaments may prefer occupying the void sites. Hence, the events involving $E_{\text{desorp, n-v}}$ or $E_{\text{desorp, n-n}}$ can be excluded. In addition, the events involving $E_{\text{neighbor-1/2/3, ox/red}}$ consider their different coordination environments for ongoing oxidation or reduction of active metals. After these KMC treatments and this KMC parameter setting, a series of KMC

simulations were carried out to dynamically reproduce the electroforming processes in nanomanipulated ECM cells with various diameters of nanopores in ion-blocking layers and void concentrations of dielectric layers in **Fig. 3**.

S2. Definition of filament diameter (D) and filament uniformity (U)

It's difficult to give a widely accepted definition for diameter of each grown filament in ECM cells, since the real filament morphology is diversified. By virtue of our KMC simulations, an approach based on the image convolution technique is developed in **Fig. S1** to grasp the important morphology characteristics of conductive filaments grown in ECM cells. The 2D grids are employed to represent the whole ECM cells. The grown filament can be regarded as grids marked by red or light red active metals here, as shown in **Fig. 1b, 3a, and 3c** of the main text. These grown filaments possess a lot of branches. They are winding, not perpendicular to the electrode surface. There are still lots of isolated clusters scattering around these grown filaments. Although all of these make the recognition of a grown filament difficult, the grid expression of this grown filament in our KMC simulations reminds us that the image convolution technique can easily recognize these gridded filaments. Finally, our developed approach can be well used to define filament diameter and filament uniformity used in **Fig. 3b** of the main text. As shown in **Fig. S1**, the snapshots of grown filaments were first taken from our KMC trajectories. Then, the first convolution realizes the image smoothing to eliminate the disperse isolated clusters around the filaments. Later, the second convolution fulfills a different image smoothing treatment to particularly smooth edges of each filament. This treatment contributes to the easy measurements of filament diameter later. Both convolution processes adopt the binarization treatment by adjusting proper convolve kernel and threshold, as shown in **Fig. S1**. After two convolution treatments, it is easy for us to finally locate the main filament. This located filament was cleaved line by line according to 2D grids, and its size can be expressed by the largest cleaved width which can be easily obtained by counting grids. Particularly, this maximum width is defined as the diameter of a grown filament in this study. Then, the filament uniformity is defined as the inverse of the standard deviation of

$$U = \sqrt{\frac{N}{\sum_{i=1}^N (D_i - \bar{D})^2}}$$

the filament width as . Noticeably, the inverse treatment here guarantees that the better uniformity corresponds to a larger value. We believe our definition here can intuitively reflect the morphology information of grown filaments. Hence, the filament diameter and filament uniformity are employed to quantify the effect of the nanomanipulation of ECM cell on filament growth.

Table S1. Parameters used in our KMC simulations.

Parameter	Value	Parameter	Value
$E_{\text{mig, v-v}}^a$	0.4 eV	$E_{\text{neighbor-1, ox}}^b$	0.49 eV
$E_{\text{mig, v-n}}$	0.6 eV	$E_{\text{neighbor-2, ox}}$	0.51 eV
$E_{\text{mig, n-v}}$	0.6 eV	$E_{\text{neighbor-3, ox}}$	0.55 eV
$E_{\text{mig, n-n}}$	0.6 eV	$E_{\text{neighbor-1, red}}$	0.36 eV
$E_{\text{desorp, v-v}}$	0.45 eV	$E_{\text{neighbor-2, red}}$	0.34 eV
$E_{\text{desorp, v-n}}$	0.45 eV	$E_{\text{neighbor-3, red}}$	0.3 eV
$E_{\text{adsorp, v-v}}$	0.38 eV	Γ_0^c	10^{12} s^{-1}
$E_{\text{adsorp, v-n}}$	0.58 eV	Valence of active metal ion	+1
$E_{\text{adsorp, n-v}}$	0.58 eV	N_c^d	6
$E_{\text{adsorp, n-n}}$	0.58 eV	σ_{metal}^e	$6.3 \times 10^7 \text{ S/m}$
$E_{\text{surf, v-v}}$	0.45 eV	$\sigma_{\text{filament}}^e$	$6.3 \times 10^6 \text{ S/m}$
$E_{\text{surf, v-n}}$	0.65 eV	σ_{iso}	$1 \times 10^{-5} \text{ S/m}$
Grid size	0.2 nm	σ_{DL}^e	$1 \times 10^{-6} \text{ S/m}$
T	300 K	$\sigma_{\text{interface}}$	$1 \times 10^{-7} \text{ S/m}$
V	2 V		

^a $E_{x, y-y}$ indicates the activation energy of different events involving in ECM cells.

^b $E_{\text{neighbor-x, ox/red}}$ corresponds to the oxidation/reduction activation energy in each case, distinguished by the number of varied neighboring active metal atoms.

Γ_0 (the approximate phonon frequency²) is taken as the preexponential factor in the Arrhenius equation and the Butler-Volmer equation to scale between real time and KMC sweeps in our KMC simulations.

^d N_c is defined as the critical nucleation volume to judge nucleation of active metal nanoclusters. After being larger than N_c for a specific newly formed nanocluster, the grids occupied by this nanocluster can surely change into void sites, and subsequently, the desorption of active metals would possibly happen for this nanocluster.

^eThe conductivity of active metal refers to that of Ag⁵, and the conductivity of dielectric layer refers to those of Si³ or SiO₂⁴. The conductivity of filament is set an order of

magnitude lower than that of the metal (σ_{metal}), because the nano-size metal filaments often have poorer conductivity.⁶

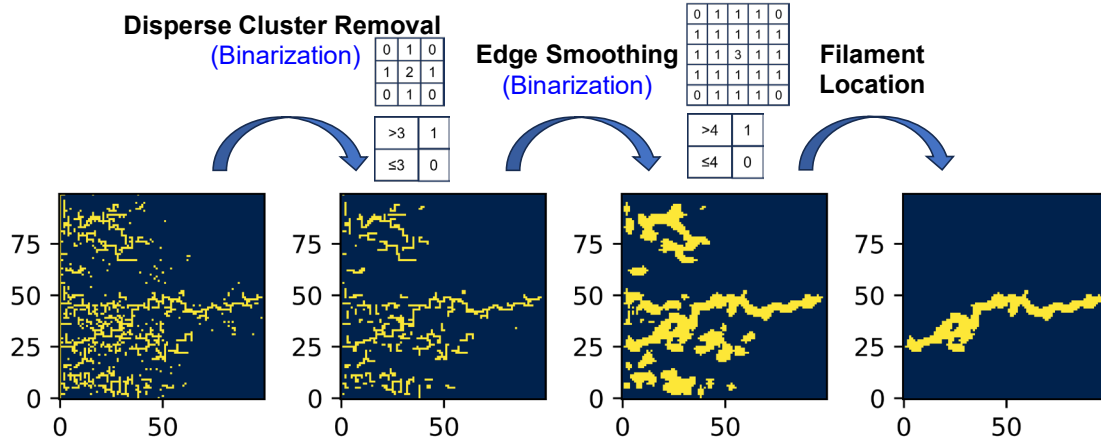


Fig. S1 Workflow of the grown filament recognition approach based on the image convolution technique. The convolve kernel and threshold used in the data processing are also present for two image convolution processes. This example was taken from the KMC trajectory of filament growth in an ECM cell with void concentration of 0.5 and without the ion-blocking layer.

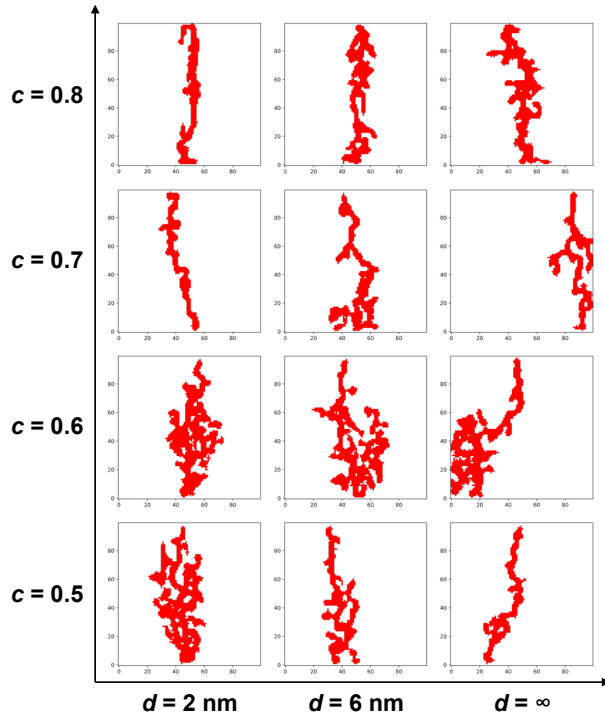


Fig. S2 Main filament recognized based on the image convolution treatments in each nanomanipulated ECM cell.

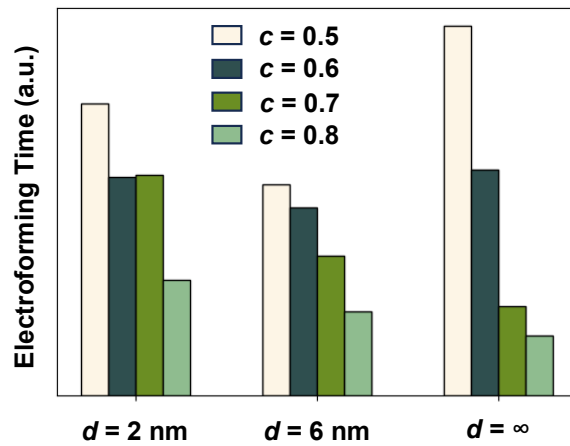


Fig. S3 Variation of electroforming time with nanopore diameter (d) and void concentration (c) for each ECM cell.

Supporting References

- 1 P. Xu, W. Fa and S. Chen, *ACS Nano*, 2023, **17**, 10511-10520.
- 2 S. Menzel, P. Kaupmann and R. Waser, *Nanoscale*, 2015, **7**, 12673-12681.
- 3 <https://www.periodic-table.org/Silicon-electrical-resistivity/> (accessed 2024-01-16).
- 4<https://matweb.com/search/DataSheet.aspx?MatGUID=ffccd1bca743445ca3bc1706a52974dd> (accessed 2024-01-16).
- 5<https://matweb.com/search/DataSheet.aspx?MatGUID=63cbd043a31f4f739ddb7632c1443d33> (accessed 2024-01-16).
- 6 S. Dirkmann, J. Kaiser, C. Wenger and T. Mussenbrock, *ACS Appl. Mater. Interfaces*, 2018, **10**, 14857-14868.